Article

Interplay of Protein Binding Interactions, DNA Mechanics, and Entropy in DNA Looping Kinetics

Peter J. Mulligan,[1] Yi-Ju Chen,[2] Rob Phillips,[3] and Andrew J. Spakowitz[1,4,5,6,*]

[1]Department of Chemical Engineering, Stanford University, Stanford, California; [2]Department of Physics and [3]Department of Applied Physics and Department of Biology, California Institute of Technology, Pasadena, California; and [4]Biophysics Program, [5]Department of Materials Science and Engineering, and [6]Department of Applied Physics, Stanford University, Stanford, California

ABSTRACT DNA looping plays a key role in many fundamental biological processes, including gene regulation, recombination, and chromosomal organization. The looping of DNA is often mediated by proteins whose structural features and physical interactions can alter the length scale at which the looping occurs. Looping and unlooping processes are controlled by thermodynamic contributions associated with mechanical deformation of the DNA strand and entropy arising from thermal fluctuations of the conformation. To determine how these confounding effects influence DNA looping and unlooping kinetics, we present a theoretical model that incorporates the role of the protein interactions, DNA mechanics, and conformational entropy. We show that for shorter DNA strands the interaction distance affects the transition state, resulting in a complex relationship between the looped and unlooped state lifetimes and the physical properties of the looped DNA. We explore the range of behaviors that arise with varying interaction distance and DNA length. These results demonstrate how DNA deformation and entropy dictate the scaling of the looping and unlooping kinetics versus the *J*-factor, establishing the connection between kinetic and equilibrium behaviors. Our results show how the twist-and-bend elasticity of the DNA chain modulates the kinetics and how the influence of the interaction distance fades away at intermediate to longer chain lengths, in agreement with previous scaling predictions.

INTRODUCTION

Genetic information is maintained and inherited by successive generations within deoxyribonucleic acid (DNA). It is not simply a repository of information through the basepair sequence. Rather, the physical properties of DNA play a key role in regulating gene expression and ultimately many key cellular and organismal processes. One of the main ways the physics of the DNA molecule enters is through looping, which allows different genomic regions to act in concert. Examples of such DNA looping processes include mating-type switching in yeast (1), genetic recombination (2), spreading of histone marks in eukaryotes (3), and supercoiling of the bacterial genome (4). In these cases, the elastic properties of the DNA molecule itself affect both the thermodynamic probability to form a loop and the kinetic lifetimes of looped configurations.

The dynamics of loop formation for general polymers has been well studied, and most theoretical work focuses on understanding the looping time (5–8) or the average time to form a loop. Much work has been done to understand how the elastic properties of semiflexible polymers like DNA (9) affect the looping kinetics (5,10,11). Experimental studies of DNA looping have looked at the cyclization rate for two ends of a chain to ligate (12–14), and from this work the Jacobson-Stockmeyer factor, or *J*-factor, is first applied to DNA looping (12,15). This approach captures the effect of the polymer chain on the equilibrium looping probability as the ratio of the rate constants for looping and unlooping. Further experimental work expands the study of DNA looping dynamics to cases where proteins, such as Lac repressor (16–18) and Fok1 (19), mediate the looping. Several theoretical studies examine the role of the protein on the kinetics (20–22). Our work builds upon the polymer physics of DNA looping and extends this to include a simple physical model for the protein that can be used to study both the looped and unlooped lifetimes.

In a previous article, we examined experiments of both the looped and unlooped lifetimes via tethered particle motion (TPM) (23). The DNA loop is mediated by the Lac repressor protein, which stabilizes the looped conformation by binding to two locations (called "operators") on the DNA. We show a dependence of the looped lifetime on the polymer energetics that is not predicted from the existing physical models of DNA looping. We explain these findings by recognizing that the loop formation process is not the same as two DNA ends fluctuating into close spatial proximity, as in cyclization experiments. The Lac repressor protein, which stabilizes the loop, has a larger range of distances for loop formation than a linear DNA chain. This interaction range has important effects on the transition state of the looping reaction and consequently the kinetics of looping and unlooping.

In this work, we use our theoretical model for DNA looping to address the kinetic behavior that results from the

Submitted March 11, 2015, and accepted for publication June 25, 2015.

*Correspondence: ajspakow@stanford.edu

Editor: Keir Neuman.

0006-3495/15/08/0618/12

http://dx.doi.org/10.1016/j.bpj.2015.06.054

physical properties of the DNA as well as those of the Lac repressor protein. Using this approach, we explore the range of behaviors that arise from varying DNA lengths and protein interaction distance. The Materials and Methods section introduces our model, which treats the looping reaction as a diffusive process on a free-energy surface. Our solution allows us to calculate not only the lifetimes of the looped and unlooped states, but also the looping *J*-factor. In Results and Discussion, we analyze the role of the interaction distance on the looping dynamics, as well as the interplay of twist and bend with varying polymer length. We also discuss how the *J*-factor does not follow from a local concentration of the ends of the polymer chain. Despite the fact that our model has been built to discuss the dynamics of protein-mediated DNA looping, the theoretical framework and underlying physical parameters are sufficiently general to allow our analysis to be applied more broadly to polymer-binding dynamics in other contexts.

MATERIALS AND METHODS

Theoretical model

We develop a molecular-level model for DNA looping and unlooping dynamics to predict the kinetics of formation and destruction of a loop within a two-site DNA-binding protein. Our theory was first brought forth to model looping kinetics in TPM experiments in a previous work (23), and the article in hand provides a detailed development and extensive analysis of the range of its behaviors. Our approach is sufficiently general to incorporate the details of different DNA-binding protein systems, as well as other DNA and non-DNA polymer looping. However, the model is sufficiently simple to render predictions of looping kinetics with minimal model parameters and without resorting to major computational simulations. A schematic of our model is provided in Fig. 1. The DNA chain is rendered as a double helix with radius and pitch consistent with B-DNA to illustrate the relative length scales within the model. However, the underlying DNA model is coarse-grained and does not incorporate the structural detail provided in Fig. 1. Here, we provide a detailed discussion of the model development and implementation.

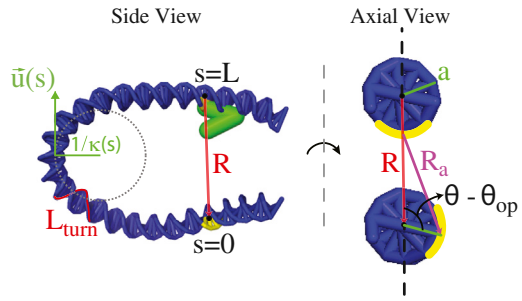

FIGURE 1 Schematic representation of our model of DNA (*blue*) and Lac repressor (*green*). The shape of the DNA chain is defined by the local tangent vector $\vec{u}(s)$ at each position s along the chain, and the local chain curvature $\kappa(s)$ is the inverse of the tangent radius. The natural DNA helicity leads to the two binding sites having a preferred twist angle θ_{op}, and the twist angle θ represents the twist deformation away from θ_{op}. The site-to-site distance R is measured from the center of the DNA chain at the two binding sites, located at positions $s = 0$ and $s = L$. The DNA chain has a radius a, and the twist angle θ results in a spatial distance R_a between the two binding sites (*yellow*). To see this figure in color, go online.

Free-energy landscape of DNA looping

Double-stranded DNA behaves as a semiflexible polymer. At short length scales, the DNA acts as a rigid rod, while at longer lengths the DNA tends to a flexible random walk in space. The wormlike chain model, which describes the polymer as an elastic strand subjected to thermal fluctuations (24), is a suitable model for DNA for short (tens of basepairs) to long lengths (thousands of basepairs), and thus spans the length scale for most transcription-factor-mediated looping motifs. Notably, experimental measurements of short DNA strands (tens of basepairs) have shown varying agreement with the wormlike chain, particularly when the DNA is highly deformed (25,26). Our goal here is to provide a simple picture of the looping kinetics, and our model can be easily modified to include a nonlinear elastic model that has been proposed for short DNA strands (9).

The bending energy for the chain is given by

$$\beta E_{\text{bend}} = \frac{l_p}{2}\int_0^L ds\left|\frac{d\vec{u}}{ds}\right|^2 = \frac{l_p}{2}\int_0^L ds\kappa(s)^2, \qquad (1)$$

where l_p is the persistence length, $\beta = 1/(K_BT)$; and L is the contour length of the chain between binding sites. The arc-length parameter s gives the position along the chain, where $s = 0$ is the position of the first binding site, and $s = L$ is the position of the second site. The curvature $\kappa(s)$ represents the change in the tangent vector as you move along the chain, such that a larger $\kappa(s)$ indicates a more locally bent configuration at position s. The tangent vector $\vec{u}(s)$ is related to the local curvature as $\kappa(s) = |d\vec{u}/ds|$. Note that we use 0.34 nm per bp to convert between length units (27). In this treatment, the twist of the chain (discussed below) is decoupled from the bending deformation. Although the coupling between twist and bend can be incorporated into the theory (28), the resulting treatment would require more details of the protein geometry and the rotational dynamics than are incorporated into our theory.

The free energy of the wormlike chain model, which includes both elastic and entropic contributions, is calculated from the Green function:

$$G(\vec{R};L) = \int \mathcal{D}[\vec{u}(s)]\delta\left[\vec{R} - \int_0^L ds\vec{u}(s)\right]\exp(-\beta E_{\text{bend}}). \qquad (2)$$

This gives the probability of the two binding sites on the DNA being separated by $\vec{R}$. Due to rotational invariance, the Green function is only a function of the separation distance $R = |\vec{R}|$ [i.e., $G(\vec{R};L) = G(R;L)$]. We use our exact solution to the Green function for a wormlike chain (28–30) and use the methods described in Mehraeen et al. (31) to calculate the Green function here. The probability of fixing the separation distance between R and $R + dR$ is given by $P(R)dR = 4\pi R^2 G(R;L)dR$, which is normalized because its integral over R is 1. The free energy of fixing the ends with separation R is given by $\beta F_{\text{conf}} = -\log[P(R)/(4\pi)]$ (removing a constant term from the factor of 4π), resulting in a conformational free energy given by

$$\beta F_{\text{conf}}(R) = -\log\left[R^2 G(R;L)\right]. \qquad (3)$$

The other contribution to the polymer energy arises from the twisting rigidity of the DNA. The formation of a looped conformation, whether for a ligation reaction between two ends of DNA or a looped structure in a DNA-protein complex, requires proper orientational alignment between the two ends. Thus, the intervening DNA of the loop may need to be twisted, with the free-energy penalty

$$\beta F_{\text{twist}}(\theta) = \frac{l_t}{2L}\theta^2, \qquad (4)$$

which is quadratic in the local twist deformation. The angle θ gives the angle of rotation about the DNA axis away from the ground-state untwisted angle, such that $\theta = 0$ is untwisted. This model assumes the twist

deformation is evenly distributed along the length of the DNA, with a twist-persistence length l_t.

We note that this model for twist is the simplest model that captures the elastic orientational penalty for deforming the chain, and thus the value of l_t could differ substantially from the intrinsic value, which has been measured as 110 nm (32). As such, it does not include the three-dimensional orientation that the two ends would need to meet; nor the entropic contributions from the twist-angle degree of freedom; nor the geometric coupling between twist and writhe of the chain. Our theory is used to model looping kinetics in TPM (23), resulting in best-fit values of the twist-persistence lengths ranging from 10 to 70 nm. In this work, we will focus on the behavior of our model in this range of values.

The undeformed orientation of the DNA is $2\pi(L/L_{\text{turn}})$, which depends upon the length of the segment to be looped due to the natural helicity of the DNA chain. The preferred twist angle, $\tilde{\theta}_{\text{op}} = 2\pi(L/L_{\text{turn}}) + \theta_0$, gives the twist angle that orients one end to face the other for binding, where θ_0 is an intrinsic angle for the orientation needed for the two ends to loop and may vary for each looping system. In our model, $\tilde{\theta}_{\text{op}}$ represents the angle to twist a given loop length to optimally align the unbound operator to dock into the free binding domain of the Lac repressor protein. We note that alignment of the orientation θ to the preferred twist angle $\tilde{\theta}_{\text{op}}$ occurs at $\theta = \tilde{\theta}_{\text{op}} - 2\pi n$, where n is any integer value. In this work, we assume n takes the value n_{min} that minimizes the twist deformation, i.e., the bound state only includes the least twisted conformation. Thus, the twist angle goes from $\theta = 0$ to $\theta = \tilde{\theta}_{\text{op}} - 2\pi n_{\text{min}}$ as the two ends are brought closer together. We define the optimal angle $\theta_{\text{op}} = \tilde{\theta}_{\text{op}} - 2\pi n_{\text{min}}$, which gives the preferred twist angle based on the minimal twist.

The separation of the two binding sites on the surface of the DNA molecule depends on the orientation. For a fixed site-to-site-distance R measured from the middle axis of the DNA strand, the actual separation R_a between the binding sites is shown in Fig. 1 and is given by

$$R_a(R,\theta) = \sqrt{(R-a)^2 + a^2 - 2a(R-a)\cos\left(\theta - \theta_{\text{op}}\right)}. \quad (5)$$

We assume that the DNA steric radius $a = 1$ nm (27).

The binding free energy drives the formation of the looped state. We choose a simple form for the energy that captures the general trend of attraction at long range and repulsion at short range, regardless of details at finer scales. We describe it with a potential well with depth ϵ_0 and an interaction length scale of δ. We also include a steric cutoff at $R = 2a$ to account for the overlap of DNA backbone segments, and thus the energy goes to infinity when R is less than this value. Our model does not rely on additional geometric parameters that may not be well characterized and may differ for each system. Thus, our conclusions are applicable to a wide range of DNA looping systems. The binding free energy is

$$\beta F_{\text{bind}}(r,\theta) = \begin{cases} \dfrac{-2\epsilon_0}{1+\exp\left[\dfrac{R_a(R,\theta)}{\delta}\right]}, & R > 2a, \\ \infty, & R \le 2a, \end{cases} \quad (6)$$

which depends on the distance between the two backbone sites R_a. Thus, the binding free energy is minimized both when the two ends are brought together (small site-to-site distance R) and when oriented appropriately ($\theta = \theta_{\text{op}}$).

The total free-energy landscape $F_{\text{total}}(R,\theta)$ shown in Fig. 2 *a* is the sum of $F_{\text{conf}}(R)$, $F_{\text{twist}}(\theta)$, and $F_{\text{bind}}(R,\theta)$. The landscape is calculated for parameters $\epsilon_0 = 23.5\ k_BT$, $\delta = 1.3$ nm, $l_p = 48$ nm, $l_t = 15$ nm, and $\theta_0 = 0.003\pi$. These parameters correspond to fits to experimental measurements for Lac-repressor mediated looping (23). The looped-state minimum occurs at $R = 2a$, and the chain has twisted to align the bindings sites, such that $\theta = \theta_{\text{op}}$. We see this progression in the twist angle in the images of DNA taken from a Monte Carlo simulation (33,34), where the color shows the twist angle going from 0 (*blue*) to $\theta_{\text{op}} = 2.16$ (*red*). We render the DNA model in these snapshots as a double helix with the appropriate radius and pitch to provide a clear perspective of the relevant length scales and twist angles throughout the looping process. The two patches of low energy near $R = 2a$ arise from either clockwise or counterclockwise rotation of the chain to align the sites, although twisting in one direction requires less total twist.

To reduce this energy surface to a single reaction coordinate (the site-to-site distance R), we calculate the minimum free-energy path from the unlooped state at point X, over the transition state Y, to the looped state Z. We calculate this minimum-path free-energy $F_{\text{min}}(R)$ by determining the value of the twist angle θ that corresponds to the minimum of F_{total} for a given value of R. In Fig. 2 *b*, we plot the minimal-path free energy, F_{min} (*black*), along with the values of F_{conf} (*green*), F_{twist} (*red*), and F_{bind} (*blue*) along this path. The minimal-path free energy serves as input to our determination of the looped and unlooped lifetimes.

Kinetic behavior from a Fokker-Planck equation

We treat the reaction from the looped to unlooped state (and vice versa) as diffusion on a one-dimensional potential energy landscape (35), given by $F_{\text{min}}(R)$ along the minimum free-energy path shown in Fig. 2 *b*.

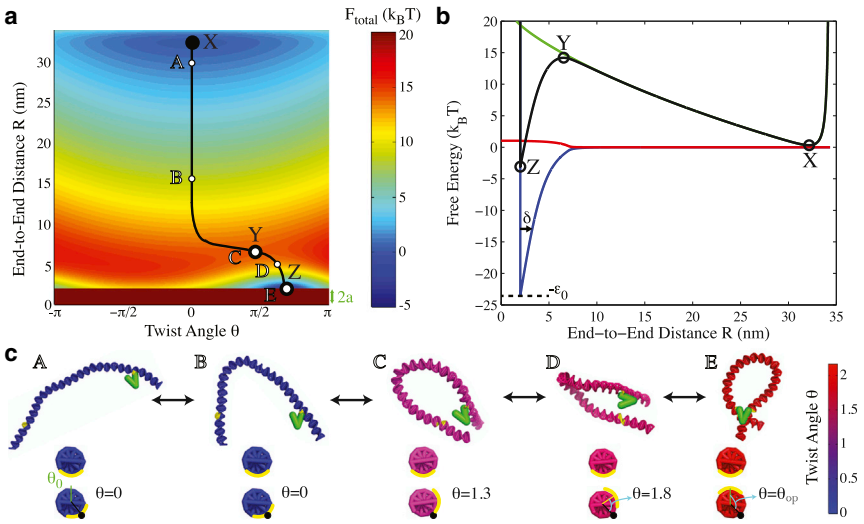

FIGURE 2 Free-energy landscape for DNA looping and unlooping. (*a*) Total free-energy surface versus site-to-site distance R and twist angle θ. (*Black curve*) Minimum free-energy path between the unlooped state (X) and the looped state (Z), passing through the transition state (Y). (*b*) Free energy along the minimum free-energy path. The minimal-path free energy F_{min} (*black*) is a combination of the conformational free-energy F_{conf} (*green*), the twisting energy F_{twist} (*red*), and the binding free-energy F_{bind} (*blue*). (*c*) Schematic of the looping reaction. The conformations are snapshots from a Monte Carlo simulation (33,34) at different site-to-site distances. The coloration shows the variation in the twist angle, and the cross-section views show θ throughout the binding process. To see this figure in color, go online.

To start, we write the Fokker-Planck equation as

$$\left(\frac{\partial}{\partial t} - \Gamma^R\right) G^R(R', t|R, 0) = 0, \tag{7}$$

where

$$\Gamma^R = D\left(\frac{\partial^2}{\partial R^2} + \frac{\partial \beta F_{\min}}{\partial R}\frac{\partial}{\partial R}\right). \tag{8}$$

The Green function $G^R(R',t|R,0)$ for the process is defined as the probability of going from a site-to-site distance R at time $t = 0$ to R' at time t. The governing Fokker-Planck equation is written using a backward representation (i.e., the Feynman-Kac formula), because we use the initial position R in this time-evolution equation. Note that we have already found the optimal twist angle θ for each site-to-site distance R, so θ does not appear explicitly in the Fokker-Planck equation. In our previous work (23), we found that $D = 8.3 \times 10^4$ nm^2/s aligns the measured looped and unlooped lifetimes to the experimental values from Lac-repressor-mediated looping. By solving Eq. 7 for free energy $F_{\min}(R)$, we calculate the flux across the transition state in either direction and the average time that is spent in either the looped or the unlooped state.

We define the survival probability $S(R,t)$ for remaining in the same state (looped or unlooped) after a given time t. When starting at a site-to-site distance R within that state, the survival probability is given by

$$S(R, t) = \int_{R_{\min}}^{R_{\max}} dR' R'^2 G^R(R', t|R, 0). \tag{9}$$

For the looped state, R is located between $R_{\min} = 2a$ and $R_{\max} = R_Y$, and for the unlooped state, the site-to-site distance R must be between $R_{\min} = R_Y$ and $R_{\max} = L$. The survival probability follows the same dynamic equation as the Green function G^R (Eq. 7), which can be obtained by performing the integration in Eq. 9. From $S(R,t)$, we calculate the first passage time $T(R) = \int_0^\infty dt S(R,t)$ as the average time to go from a site-to-site distance R to the transition state at $R = R_Y$. Following from Eq. 7, we write

$$\Gamma^R T = D\left(\frac{\partial^2 T}{\partial R^2} + \frac{\partial \beta F_{\min}}{\partial R}\frac{\partial T}{\partial R}\right) = -1, \tag{10}$$

with boundary conditions of $T(R = R_Y) = 0$ for both the looped and unlooped states, $(\partial T/\partial R)(R = 2a) = 0$ for the looped state, and $(\partial T/\partial R)(R = L) = 0$ for the looped state. By letting $\Phi = \partial T/\partial R$, we can solve the resultant first-order ordinary-differential equations with an integrating factor. Finally, we average $T(R)$ over all possible starting site-to-site distances to obtain the mean looped and unlooped lifetimes. The mean looped lifetime is given by

$$\langle \tau_{\text{loop}} \rangle = \frac{1}{DQ_{\text{loop}}} \int_{2a}^{R_Y} dR \int_{R}^{R_Y} dR' \times \int_{2a}^{R'} dR'' e^{-\beta F_{\min}(R) + \beta F_{\min}(R') - \beta F_{\min}(R'')}, \tag{11}$$

where the looped state ranges from $R = 2a$ to $R = R_Y$, and the mean unlooped lifetime is

$$\langle \tau_{\text{unloop}} \rangle = \frac{1}{DQ_{\text{unloop}}} \int_{R_Y}^{L} dR \int_{R_Y}^{R} dR' \times \int_{R'}^{L} dR'' e^{-\beta F_{\min}(R) + \beta F_{\min}(R') - \beta F_{\min}(R'')}, \tag{12}$$

where the unlooped state ranges from $R = R_Y$ to $R = L$. We define the partition function for the looped state as $Q_{\text{loop}} = \int_{2a}^{R_Y} dR \exp[-\beta F_{\min}(R)]$ and the unlooped-state partition function as $Q_{\text{unloop}} = \int_{R_Y}^{L} dR \exp[-\beta F_{\min}(R)]$.

From our model, we calculate the J-factor for the looping reaction. This quantity is defined as the exponential of the free-energy difference between the looped and unlooped states for the polymer chain only, as discussed in previous work (23,36,37). The J-factor is given by

$$J_{\text{loop}} = (1\text{ M})\exp\left[-\beta\left(F_{\text{poly}}^{\text{loop}} - F_{\text{poly}}^{\text{unloop}}\right)\right], \tag{13}$$

where we assume a standard state of 1 M, as in previous treatments (23,36,37). Our definition of the J-factor in Eq. 13 incorporates the shape of the entire free-energy surface, incorporating both entropic and energetic effects. In J-Factor Comparison, we demonstrate that our model results in nonideal J-factor predictions that correlate with but are quantitatively distinct from an ideal interpretation of the J-factor as an effective concentration. The free energies $F_{\text{poly}}^{\text{loop}}$ and $F_{\text{poly}}^{\text{unloop}}$ only include the energetic contributions from the polymer chain configuration and do not include the binding interaction. We write

$$F_{\text{poly}}^{\text{loop}} = -k_B T \log Q_{\text{loop}} - \frac{\int_{2a}^{R_Y} dR F_{\text{bind}}(R)\exp[-\beta F_{\min}(R)]}{Q_{\text{loop}}}, \tag{14}$$

where the first term captures the total free energy of the looped state and the second term removes the binding energy contribution from $F_{\text{bind}}(R)$. We similarly write

$$F_{\text{poly}}^{\text{unloop}} = -k_B T \log Q_{\text{unloop}} - \frac{\int_{R_Y}^{L} dR F_{\text{bind}}(R)\exp[-\beta F_{\min}(R)]}{Q_{\text{unloop}}}. \tag{15}$$

Equations 14 and 15, when put into Eq. 13, allow us to calculate J_{loop}.

RESULTS AND DISCUSSION

The model developed above connects the kinetics of polymer looping to the free energy of the polymer chain and the binding interactions. This accurately reflects the behavior of shorter chains, where the limiting rates for loop formation are governed by the high energetic costs for bending and twisting the chain. The results of these calculations reveal the strength of the coupling between the looping dynamics of these short chains and the physical forces associated with the polymer rigidity and the binding interactions.

Effect of the interaction range

Forming a loop in DNA (e.g., DNA cyclization (12–14)) requires one end to enter into the vicinity of the other. The probability of the polymer having a conformation that allows binding is described by the J-factor, which was first described by Jacobson and Stockmayer (15) in their work on ring formation in polycondensation reactions. Since then, the J-factor has been applied to the cyclization probability of DNA (12–14) as well as protein-mediated looping

probabilities (36,37). These experiments measure the *J*-factor from the ratio of the association and dissociation rates for ring or loop formation, resulting in its measure as a concentration. This ratio is proportional to the exponential of the free-energy difference for the polymer chain between the looped and unlooped states, and essentially accounts for the probability of the polymer adopting a potential binding conformation given the associated entropic and elastic costs.

In Eqs. 14 and 15, we describe the calculation of the free-energy difference for the polymer chain from the free-energy landscape. The *J*-factor calculated from our model is plotted in Fig. 3 *a*. For now, we just consider the black curve, whose parameters are chosen based on our fits to the experimentally determined loop lifetimes (23), with $\delta = 1.3$ nm, $\epsilon_0 = 23.5\ k_BT$, $\theta_0 = 0.03$, and $l_p = 48$ nm. Throughout this section, we only discuss our model without twist (i.e., $l_t = 0$) and defer our discussion of twist to the following sections. At short lengths, the *J*-factor is small primarily because of the high elastic energy penalty to bring the DNA into the looped shape (38). It reaches a peak value

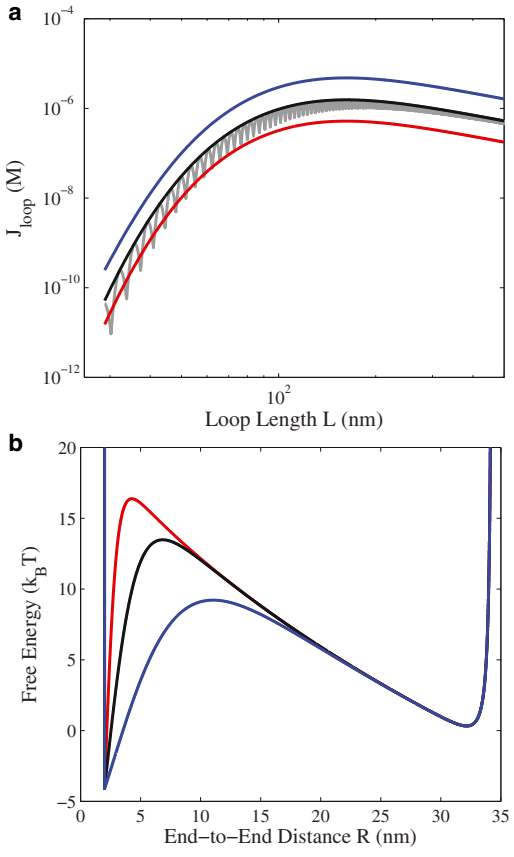

FIGURE 3 Interaction distance shifts the *J*-factor and the transition state. (*a*) Looping *J*-factor plotted versus loop length, for a chain with $\epsilon_0 = 23.5\ k_BT$, $l_p = 48$ nm, and $\theta_0 = 0.003\pi$. We vary δ from 0.5 nm (*red*) to 1.3 nm (*black*) to 3 nm (*blue*) with the twist-persistence length $l_t = 0$ nm. (*Gray*) We plotted $\delta = 1.3$ nm but with $l_t = 15$ nm. (*b*) Free energy F_{min} versus site-to-site distance for a strand of length $L = 101$ bp, with all other parameters the same as in (*a*). To see this figure in color, go online.

where $L \approx 3.4l_p$, matching results of other calculations (28,38). At longer lengths, the *J*-factor begins decreasing again because the entropic penalty for keeping a short site-to-site distance is more thermodynamically significant than the reduced penalty from the bending energy.

One of the major features of our model is the presence of an interaction distance δ that allows the binding energy to be felt from larger site-to-site distances. Decreasing this interaction distance shifts the transition state's site-to-site distance R_Y to the left, as is seen in Fig. 3 *b*. Here, we plot the free energy along the minimal path $R_{min}(R)$ at three different values of the interaction distance: 3 nm (*blue*), 1.3 nm (*black*), and 0.5 nm (*red*). All other parameters are set to the same values as in the black *J*-factor curve in Fig. 3 *a*. At small values of δ, the transition state occurs at a separation that is only marginally larger than the looped state conformation. With a smaller range of site-to-site distances and a larger barrier to clear the transition state, the polymer free energy F_{poly}^{loop} of the looped state rises, and accordingly the *J*-factor decreases (as per Eq. 13).

In Fig. 3 *a*, we also plot the *J*-factor for $\delta = 3$ nm (*blue*) and $\delta = 0.5$ nm (*red*), with the other parameters the same as in the black curve. The increased interaction range, from 1.3 nm to 3 nm, results in the *J*-factor shifting up by a multiplicative factor of 3.08 (for lengths past the maximum *J*-factor). The shift from 0.5 to 1.3 nm is 2.99. We note that although the interaction distance is a property of the protein and its binding potential, it enters into the measured *J*-factors by its effect on the total free energy.

In Fig. 4, we plot the looped and unlooped lifetimes versus length for the same three values of the interaction distance δ as for the *J*-factors in Fig. 3 *a*. The relationship between length and lifetime is presented in Fig. 4 because this is the experimentally measured relationship and is consistent with how the *J*-factor is typically presented. These curves show the looped lifetime increasing with increasing loop length, and conversely, the unlooped lifetimes decrease with loop length. While length can be a useful measure of the polymer flexibility, it does not account for changes in other properties, such as the persistence length, which can influence the probability of the polymer forming a looped conformation. The *J*-factor captures all of the contributions of bending and twisting within our model, and we can plot the lifetimes versus the *J*-factor to understand how the polymer behavior affects the rates of looping and unlooping. The ratio of the looped and unlooped lifetimes is the *J*-factor (i.e., $\langle\tau_{loop}\rangle/\langle\tau_{unloop}\rangle = J_{loop}$). The *J*-factor is viewed as the local end concentration (12,39) and appears as a reactant within the statistical weight for the looped complex in a model for Lac-repressor looping (23,40). Based on this argument, we would expect the *J*-factor to largely correlate with the unlooped lifetime (i.e., the association rate of the two ends).

However, experimental measurements of the looped lifetime showed a surprising dependence upon the looping

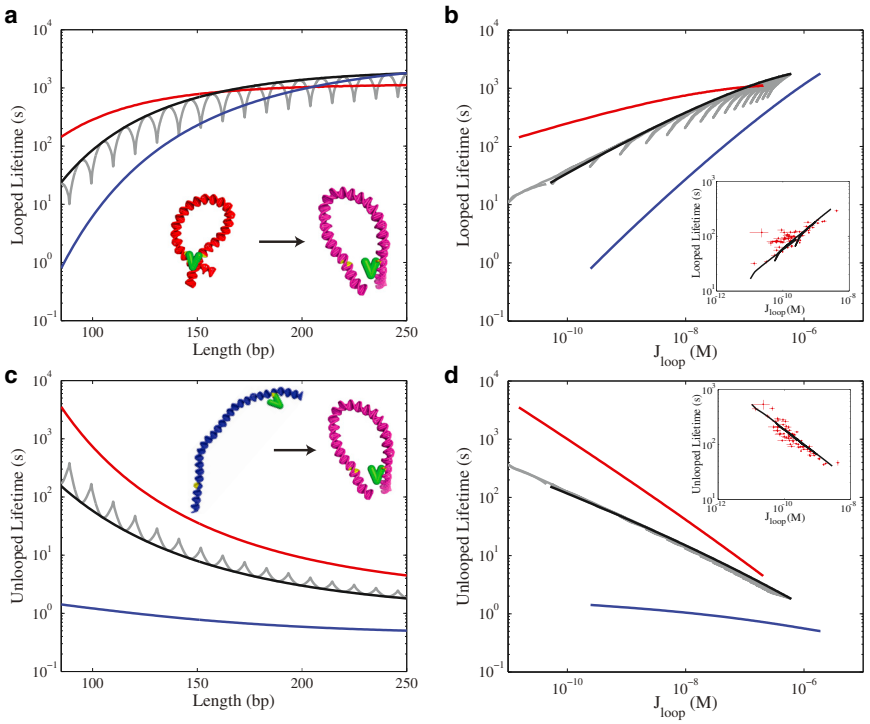

FIGURE 4 Looped and unlooped lifetimes. (*a*) Looped lifetimes plotted versus loop length. We vary δ from 0.5 nm (*red*) to 1.3 nm (*black*) to 3 nm (*blue*) with the twist-persistence length l_t = 0 nm (see text for other parameter values). (*Gray*) We plot $\delta = 1.3$ nm but with $l_t = 15$ nm. (*b*) Looped lifetimes versus *J*-factors for DNA chains running from lengths of 85 to 250 bp with the same parameters and colors as in (*a*). (*Inset*) Comparison between our theory (with $\delta = 1.3$ nm and l_t = 15 nm) and TPM experiments from Chen et al. (23). (*c*) Unlooped lifetimes versus length, with the same parameters as in (*a*). (*d*) Unlooped lifetimes versus *J*-factors, with the same parameters as (*a*). (*Inset*) Comparison between our theory (with $\delta = 1.3$ nm and $l_t = 15$ nm) and TPM experiments from Chen et al. (23). To see this figure in color, go online.

J-factor (23). In Fig. 4 *a*, we plot the looped lifetime $\langle\tau_{\text{loop}}\rangle$ versus length, and in Fig. 4 *b*, we show the looped lifetime versus the *J*-factor, over the same range of lengths (85–250 bp) as in Fig. 4 *a*. The colors correspond to the same three values of the interaction distance δ as shown in Fig. 3. The inset to Fig. 4 *b* shows a comparison between the looped lifetime from our theory (with $\delta = 1.3$ nm and $l_t = 15$ nm) and the TPM experimental data found in Chen et al. (23). The agreement between our theory and the TPM experiments suggest the value $\delta = 1.3$ nm is the experimentally relevant value. We argue that the interaction length scale δ plays a key role in the looped lifetime dependence on the *J*-factor (23). Larger values of the interaction distance δ shift the location of the transition state R_Y to larger site-to-site distances, as seen in Fig. 3 *b*. When the transition-state distance R_Y is much larger than the looped state distance R_X, there is a significant release of elastic deformation of the chain going from the looped state to the transition state. We see the shift in the dependence of the looped lifetime on the interaction distance in Fig. 4 *b*. As we decrease δ from 3 nm (*blue*) to 0.5 nm (*red*), the slope of the looped lifetime gradually goes away, as does the dependence of the looped lifetime on the elastic properties of the polymer.

The *J*-factor still correlates with the kinetics of association (i.e., the unlooped lifetime). In Fig. 4 *c*, we show the unlooped lifetimes versus length, and in Fig. 4 *d*, we plot the unlooped lifetimes versus J_{loop} over the same length ranges as in Fig. 4 *c*. The inset to Fig. 4 *d* shows a comparison between the unlooped lifetime from our theory (with $\delta = 1.3$ nm and $l_t = 15$ nm) and the TPM experimental data found in Chen et al. (23). Because J_{loop} is part of the association reaction statistical weight, we would have assumed, treating J_{loop} as a concentration in a first-order reaction, that the reaction rate for leaving the unlooped state would be proportional to J_{loop}. Thus, the unlooped lifetime would be inversely proportional to the *J*-factor. Instead, we see that although the unlooped lifetime decreases with increasing *J*-factor, the relationship is less pronounced than $\tau_{\text{unloop}} \propto J^{-1}{}_{\text{loop}}$.

We quantify the dependence of the lifetimes on the *J*-factor by measuring the scaling exponents *b* and *c* for a fit of $\tau_{\text{loop}} \propto J^b$ and $\tau_{\text{unloop}} \propto J^c$. We perform the fit for lengths *L* varying from 185 to 225 bp to ensure we are within a length regime behaving as a power law. The scaling *b* of the looped lifetime ranges from 0.1032 (*red*, $\delta = 0.5$ nm) to 0.3072 (*black*, $\delta = 1.3$ nm) to 0.7147 (*blue*, $\delta = 3$ nm). Meanwhile, the scaling of the unlooped lifetime with *J* also increases with δ, going from −0.7451 (*red*) to −0.5361 (*black*) to −0.1662 (*blue*). The difference between the looped and unlooped scaling exponents is ~1, as expected by the ratio of the looped to unlooped lifetimes being proportional to the *J*-factor.

The predicted dependence of the lifetimes on the *J*-factor arises from the shape of the governing free-energy F_{min}. For the length $L = 101$ bp in Fig. 3 *b*, increasing δ from 0.5 to 3 nm results in a shift in the transition-state position R_Y toward larger values, resulting in a reduction in the transition-state free energy due to a reduction in the conformational free-energy F_{conf}. Shorter chains will exhibit a larger

degree of reduction of the transition-state free energy than larger chains, leading to a length-dependent transition-state free energy. Because the looped and unlooped lifetimes in Fig. 4 are dictated by the transition-state free energy, the shift in the position of the transition state and the resulting free-energy change will dramatically affect the lifetimes. The influence of δ on the position of the transition state is the root cause of the observed scaling of the lifetimes versus the J-factor.

Thus far, we only discuss the behavior for $l_p = 48$ nm, corresponding to the approximate value of the DNA persistence length. It is now illustrative to explore the impact of bending rigidity on the looping kinetics, both for fundamental insight and for addressing the impact of changes in sequence in modulating the behavior. If we increase the persistence length, the increased resistance to bending results in the looped state experiencing greater elastic resistance, and the conformational free energy from Eq. 3 (plotted in *green* in Fig. 2 *b*) starts increasing more sharply as the two ends come together. Consequently, the release of elastic stress from the looped state to the transition state is higher, and we therefore expect the scaling dependence to be inversely proportional to the persistence length. This results in a balance between the length scale of the elastic stiffness and the length scale of binding, affecting the transition-state location and the kinetic lifetimes.

We consider persistence lengths varying from 40 nm (*blue*) to 48 nm (*green*) to 55 nm (*red*) and interaction radii varying from 0.1 to 8 nm. The scaling exponents b for the looped (*solid lines*) and unlooped (*dotted lines*) lifetimes are plotted in Fig. 5 versus the ratio of the interaction range over the persistence length δ/l_p. We calculate the exponents from values of the DNA length ranging from 120 to 150 bp for a chain with no twist ($l_t = 0$), $\epsilon_0 = 23.5\ k_BT$, and $\theta_0 = 0.003\pi$. Except when δ is very large, the curves fall on the same curve, showing that the dependence on the J-factor is due to the balancing between the binding interaction length scale and the elastic deformation length scale. Deviations at large δ occur because of the diffusion timescale, as it leaves the looped state, exceeding the timescale for crossing the energetic barrier. Because the ratio of the looped to the unlooped lifetimes are proportional to J^1, the difference between the scaling laws remains ~1. For small values of δ/l_p, the scaling exponent for the looped lifetimes goes to zero, and the scaling exponent for the unlooped lifetime approaches 1, because the looped lifetime becomes independent of the J-factor.

The role of twist elasticity

The general dependence of the looping dynamics on the elastic energy within the polymer is determined by the bending energy. Similarly, the behavior of the J-factor over many helical repeat lengths is largely dictated by the bending energy. However, the twist resistance enters into the behavior and is the dominant factor in modulating the J-factor over a short range of DNA lengths (28,36). Because the helical repeat length L_{turn} of DNA is only 10.46 bp, the addition of just 5 bp can shift the orientation almost 180°. Fig. 6 gives values of the relaxed orientation angle θ_{op} and the corresponding bend-and-twist free energies over a single helical repeat. Thus, over short lengths, the twist free energy needed to align the DNA ends for appropriate binding (Eq. 4 evaluated at $\theta = \theta_{\text{op}}$) can shift from a minimum of 0 when the DNA does not need to twist from its natural orientation to orient the two ends properly, to a maximum when $\theta_{\text{op}} = \pi$.

The twist angle θ needed to align the ends affects the J-factor, which measures the free-energy change from the unlooped state to the looped state. Being in the looped state

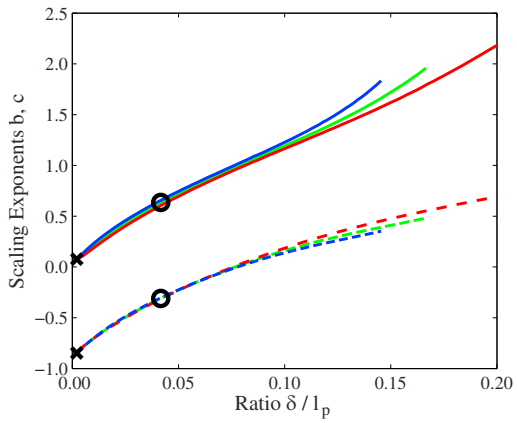

FIGURE 5 Scaling dependence versus J-factor. Scaling exponents b (*solid curves*) and c (*dashed curves*), where $\tau_{\text{loop}} \propto J^b$ and $\tau_{\text{loop}} \propto J^c$, versus δ/l_p for three different persistence lengths: 40 nm (*blue*), 48 nm (*green*), and 55 nm (*red*). (*Crosses* and *circles*) Points described in the text. To see this figure in color, go online.

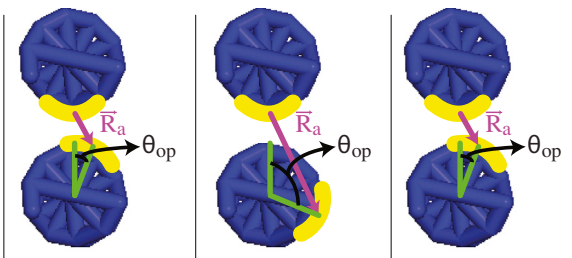

L	95 bp	100 bp	105.46 bp
θ_{op}	0.114 π	0.624 π	0.114 π
F_{twist}	0.198 k_BT	5.658 k_BT	0.178 k_BT
F_{conf}	20.198 k_BT	19.535 k_BT	18.785 k_BT

FIGURE 6 Table showing the change in the relaxed orientation angle θ_{op} and bend-and-twist free energies at three different lengths. To see this figure in color, go online.

requires the polymer to not only bend into a close site-to-site distance, but also to twist in order to allow the ends to bind. The addition of twist free energy lowers the J-factor from the no-twist state (*black curve* in Fig. 3), with greater deviation with increasing DNA twist at half-integer turns. We plot the J-factor with twist (for $l_t = 15$ nm) in gray. The oscillations in the J-factor have a periodicity of L_{turn} due to the orientation changing through an angle of 2π over that length. The deviation from the black curve is strongest at short lengths, because the twist deformation is assumed to spread equally over the full length of the chain. At long lengths, these oscillations disappear. The presence of twist deformation also affects the looped and unlooped lifetimes, as shown by the gray curves in Fig. 4. We see deviations from the black curves as the twist angle needed for the preferred binding orientation oscillates away from zero. Additionally, the one-to-one dependence between J-factor and the looped lifetime no longer holds.

When there is no penalty for twisting ($l_t = 0$), the DNA chain is free to take any twist angle θ and thus assume $\theta = \theta_{\text{op}}$ at all site-to-site distances R. With twist resistance, the angle changes from $\theta = 0$ to $\theta = \theta_{\text{op}}$ as diagrammed in Fig. 2 *c*. The twist free energy primarily affects the looped state, as the DNA chain only begins to twist when it feels the favorable binding energy associated with orienting toward the other end, as shown in the red curve in Fig. 2 *b*. Because the twist free energy only starts to increase for site-to-site distances smaller than the transition state at R_Y, only the energy barrier to leave the looped state is affected. The scaling law no longer holds for the looped lifetimes because the energy barrier for the looped lifetime and the J-factor increase proportionally to twist, so the scaling over lengths <1 twist oscillation look more like ${J^1}_{\text{loop}}$.

We can see these effects clearly in Fig. 7 *a*, where we have plotted the looped (*red*) and unlooped (*blue*) lifetimes for lengths ranging from 84 to 135 bp, with $\delta = 0.1$ nm, $l_t = 50$ nm, and all other parameters the same as previously defined. In this plot, we use the elevated value $l_t = 50$ nm to accentuate the oscillations arising from twist deformation. The interaction distance $\delta = 0.1$ nm is very small, and the scaling exponent b for the looped lifetime without twist should be nearly 0, as indicated by the red dashed line and the crosses in Fig. 5. The unlooped lifetime without twist should be nearly proportional to ${J^{-1}}_{\text{loop}}$, which is indicated by the blue dashed line. The free-energy barrier of the looped state and the J-factor are both dependent upon the twist free energy, which changes sharply with length, and the bending energy changes only mildly with length over a short length range. Thus, the looped lifetime over a single decade shows a scaling law closer to ${J^1}_{\text{loop}}$ (*black dotted line*). Because both the twisting and bending free energies are slightly dampened as you increase length, the scaling exponent looks a bit less than 1. On the other hand, because the energy barrier to leave the unlooped state is largely unaffected by the twist, the unlooped lifetime over these short

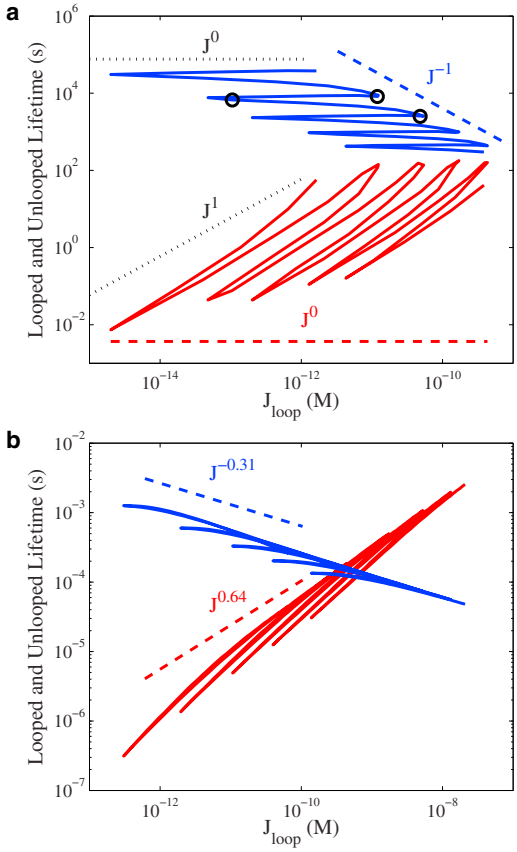

FIGURE 7 Twist influence on looped and unlooped lifetimes. (*a*) Looped (*red*) and unlooped (*blue*) lifetimes for a DNA chain with persistence length of 48 nm, $\epsilon_0 = 23.5\ k_BT$, $\theta_0 = 0.003\pi$, $\delta = 0.1$ nm, and $l_t = 50$ nm. The loop lengths range from 85 to 135 bp. (The *three circles* are the DNA lengths in Fig. 6; the scaling behavior for the *dashed lines* is from the *crosses* in Fig. 5.) (*b*) Looped (*red*) and unlooped (*blue*) lifetimes for DNA chain with the same parameters as in (*a*) except the interaction distance is $\delta = 2$ nm. (Scaling behavior for the *dashed lines* is taken from the *circles* in Fig. 5.) To see this figure in color, go online.

lengths follow a scaling that looks more like ${J^0}_{\text{loop}}$ (*black dashed line*). Over many decades in length, the twist energetic penalty continues oscillating to smaller and smaller values, while the elastic bending resistance steadily decreases and is the dominant effect. Thus, over long lengths, the lifetimes follow the scaling trends without twist that are given in Fig. 5 *a*.

The same general behavior is shown in Fig. 7 *b*, where we plot the same polymer system as in Fig. 7 *a* except for an interaction distance $\delta = 2$ nm. The scaling laws for the no-twist deformation case are given for the looped (*red dashed line*) and unlooped (*blue dashed line*) lifetimes, taken from the values circled in Fig. 5. The curves plotted here come much closer to a one-to-one correspondence between the J-factor and the kinetic lifetimes. This occurs because the looped and unlooped lifetime scalings due to the bending resistance alone (as shown in Fig. 5) nearly match up with the slope at short length scales that is due

to the twist oscillations. Thus, while certain values of the interaction radius could make the relationship appear to be a universal trend, the overall behavior of the *J*-factor cannot capture in a one-to-one relationship the lifetimes of the looped and unlooped states.

J-factor comparison

The effect of the protein properties on the *J*-factor challenges the conventional view of the *J*-factor as capturing the local concentration of one end of the polymer chain at the other end, which is calculated based on the site-to-site distribution of the polymer chain. We write this local concentration as

$$J_{\text{conc}} = \frac{10\ \text{nm}^3\text{M}}{6.02} \lim_{x\to 0} \frac{4\pi}{L^3} \frac{\int_0^x dR R^2 G(R)}{\frac{4}{3}\pi x^3} = \frac{10\ \text{nm}^3\text{M}}{6.02} \frac{G(R=0)}{L^3}, \quad (16)$$

where $G(R)$ is the Green function for the site-to-site distance defined in Eq. 2. The numerator captures the probability of the two ends being within distance x of each other, and the denominator is the volume encapsulated by the sphere of reaction radius x. Taking the limit gives us the local concentration at $R = 0$. The factor of 10 nm^3 M/6.02 comes from converting the units from 1 chain per nm^3 (assuming L has units of nm) to M.

In Fig. 3 *a*, we show that the *J*-factor is dependent on the value of the interaction radius δ. However, the limit of $x \to 0$ in Eq. 16 has no dependence on δ. Thus, J_{loop} (from Eq. 13) does not have a simple correspondence to the local concentration at $R = 0$. Given that the looping reaction is not required to happen within a very small reaction window (41–43), a more appropriate view of the *J*-factor might be the concentration of the other end within a larger sphere (i.e., $x \neq 0$). This approach is first used in Douarche and Cocco (22) to show how the *J*-factor could be modulated by orders of magnitude given a large capture radius. In their work, they adjusted the capture radius x to account for the effect of protein size on the *J*-factor of a wormlike chain.

We adjust Eq. 16 and not take the limit to zero, instead choosing some reaction radius x that it would need to be in to form a loop. Our calculation uses the full analytical solution to the Green function for the wormlike chain (28,31), which was unavailable at the time that Douarche and Cocco (22) did their work. We see close quantitative agreement between our results, plotted in red in Fig. 8, and their calculations extending the saddle-point approximation of Shimada and Yamakawa (38) in Fig. 4 of Douarche and Cocco (22). The solid line ($x = 1.3$ nm) and the dashed line ($x = 5$ nm) converge to a single curve at larger values of loop length.

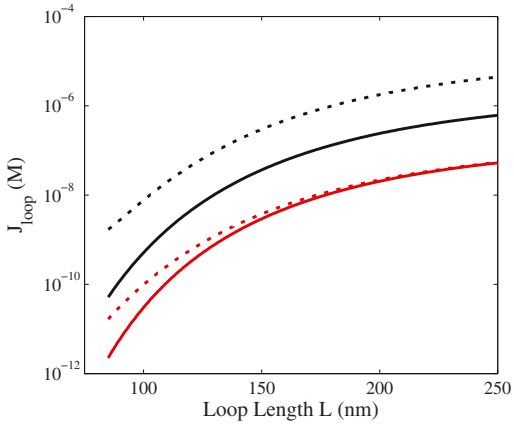

FIGURE 8 *J*-factor versus length. (*Black lines*) Plots of J_{loop}, as calculated in Eq. 13, for a DNA chain with the same properties as in Fig. 2 and $\delta = 1.3$ nm (*solid*) or $\delta = 5$ nm (*dashed*). (*Red curves*) The *J*-factor without taking the limit of reaction radius x to zero, as defined in Eq. 16. (*Solid lines*) $x = 1.3$ nm; (*dashed lines*) $x = 5$ nm. To see this figure in color, go online.

This convergence is qualitatively different from the behavior of J_{loop}, plotted in Fig. 3 *a*. We plot J_{loop} as defined in Eq. 13 for $\delta = 1.3$ nm (*solid black*) and 5 nm (*dashed black*). The impact of the binding energy and the protein properties on the *J*-factor persists at long lengths. Thus, the *J*-factor measured in experiments as a free-energy difference between the looped and unlooped states have qualitative distinctions from the local end concentration of the polymer chain.

Behavior at intermediate lengths

The *J*-factor, and thus the looping probability, peaks at chain lengths that are a few persistence lengths long. In the limit of long chain length, the wormlike chain model behaves as a Gaussian or flexible chain, with conformations that behave as a random walk in space. We plot the dependence of the looped and unlooped lifetimes for lengths spanning from 85 to 4500 bp in Fig. 9, with the same parameters as in Fig. 3. As before, we see that the looped lifetimes increase with length for shorter length chains while the unlooped lifetimes decrease with length. However, at the DNA length at which the *J*-factor reaches its maximum (479 bp or ~163 nm), the unlooped lifetime begins to increase with length, and the looped lifetime levels off and remains the same regardless of length. In the plots, we show that this behavior is true regardless of the interaction length δ. Thus, the polymer goes to the same scaling at these longer lengths regardless of the short-length scaling, which is shown to be dependent upon the value of δ.

At these intermediate length DNA chains, the elastic barrier to loop formation is no longer the dominant barrier and thus the release of elastic strain in going from the looped state to the transition state plays only a minimal role. As such, at lengths beyond the peak value of *J*-factor, the

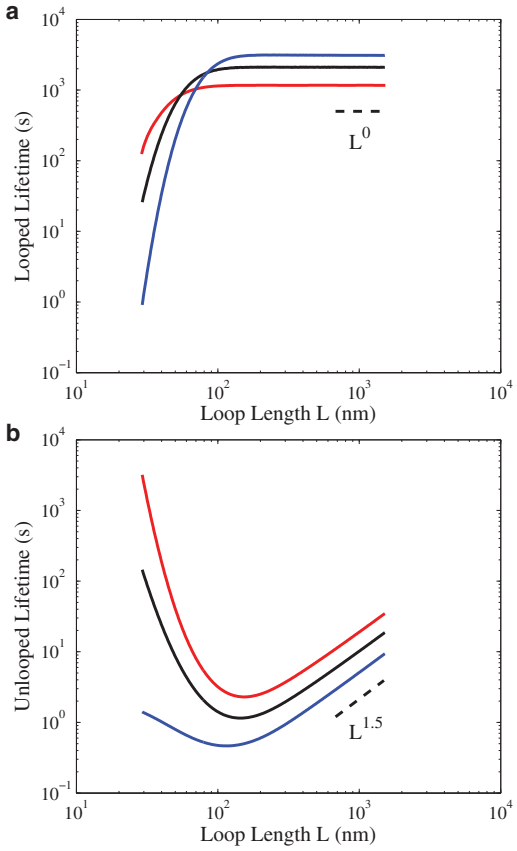

FIGURE 9 Behavior of looped and unlooped lifetimes at intermediate lengths. (*a*) Looped lifetimes versus length for DNA chains running from 85 to 4500 bp. All curves are for a chain with $\epsilon_0 = 23.5\ k_BT$, $l_p = 48$ nm, and $\theta_0 = 0.003\pi$. The interaction distance varies with $\delta = 0.5$ nm (*red*), $\delta = 1.3$ nm (*black*), and $\delta = 3$ nm (*blue*). The scaling law shows the behavior at larger values of length. (*b*) Unlooped lifetimes versus length, with all the same parameters as in (*a*). To see this figure in color, go online.

looped lifetime becomes independent of both J_{loop} and the loop length L. The unlooped lifetime reaches a scaling with length of $L^{1.5}$, as shown in Fig. 9 *b*. This is consistent with predictions using the Gaussian chain model for the unlooped lifetime (7,8). At some larger length, however, the looped and unlooped lifetime behaviors exhibited in Fig. 9 break down, as the kinetics no longer are governed by the energetic barriers but depend upon the relaxation of the polymer chain. Other work has looked into this crossover and found that the unlooped-lifetime scaling shifts from 1.5 to 2, which is characteristic of the relaxation time for a Rouse chain (8). The length at which the Rouse relaxation time begins to dominate the looping kinetics by becoming slower than the local equilibration time has been calculated to be tens of persistence lengths (it is dependent upon the capture radius as well) (8). Our model does not account for the effects of polymer relaxation, and therefore, the Rouse scaling of L^2 will not be predicted by our model in the large length limit. We restrict our discussion to short and intermediate chain lengths where the assumption of local equilibrium is valid.

CONCLUSIONS

One of the surprising results of the experimental measurements of the lifetimes of Lac repressor-mediated loops is the dependence of the looped lifetime on the *J*-factor. A view of the *J*-factor within the statistical mechanical framework of looping dynamics suggests that the effects of the polymer chain properties should be confined to influencing the association reaction alone, and most theoretical work on looping dynamics has focused on the unlooped lifetime dependence upon the polymer length and properties (6,8,11,44,45). Dissociation rates have typically been thought of as only involving the separation of the binding surfaces at the interface between them and thus would not involve larger-scale events dependent on polymer conformation (16–19). With a simple model of a semiflexible polymer and a binding interaction with a finite length scale, we have shown how the *J*-factor can influence both the looped and unlooped lifetimes.

The dependence of the looped and unlooped lifetimes on the *J*-factor is primarily captured in our model by the binding potential. The shape of this interaction energy influences the distribution of states that the DNA and protein adopt within the "looped state", which refers to all the site-to-site distances shorter than the transition state at R_Y. The main factor that influences the shape of the binding energy is the interaction distance δ. Physically, this parameter captures the range of the binding energy, i.e., how far away the two ends are when they start to feel each other and consequently be influenced to approach and form a loop. At further distances, the two binding sites have a weak interaction, and the favorable binding energy decreases as the two ends approach each other.

Several factors contribute to why we model the binding energy this way and what should contribute to the magnitude of δ. On an atomic scale, the favorable electrostatic interactions that govern binding increase as the two ends are brought together. For a protein-mediated loop process, such as that of Lac repressor, the protein size (41) and flexibility (42) play an additional role. The size of a protein and the location of the binding domains affect the shape of the preferred looped conformations and the polymer site-to-site distances at which binding occurs. Internal flexibility of the protein can allow the binding sites to stretch with some energetic cost, resulting in the DNA feeling the binding interaction before it reaches the fully bound state. Finally, the binding domains on the protein may nonspecifically bind to the DNA and slide along the DNA before docking into the binding site (43), effectively extending the range of lengths where the binding interactions occurs.

Our model, using δ to modulate the shape of the binding well, captures these effects in the simplest manner possible.

More detail could be added to properly account for the sterics and features of the protein within the looping reaction, as in Villa et al. (21) and Zhang et al. (46), as well as separate interaction energies for nonspecific binding of the DNA. While these would perhaps add to the quantitative accuracy for various systems, the qualitative features captured by simply recognizing the distance-dependent effects of the binding interaction provide an intuitive view of how the polymer physics impacts both the association and dissociation reactions.

The J-factor is captured experimentally through the looping probabilities (12–14,36,37) and is a measure of the free-energy difference of the polymer chain between the looped and unlooped states. While the J_{loop} term appears as if it is a local concentration within the kinetic framework, it cannot be reconciled as such because the shape of the binding energy affects the free energy of the looped state. In order to obtain the J-factors of previous works that have looked at protein size affecting the reaction radius (22,47), we would need to assume a constant binding energy well within the looped state.

One of our major findings is that the scaling we observe for the looped and unlooped lifetimes versus the looping J-factor is dependent upon the balance of the bending energy (modulated by the persistence length) and the interaction length scale δ. As the length of the polymer chain increases, the impact of the bending free energy diminishes, and the increased flexibility decreases the looped state free energy. However, the location of the transition state dictates the fraction of the bend energy that is alleviated between the looped state and the transition state. If δ is very small, the bending-energy difference between the looped state and the transition state is negligible, and the looped lifetime is independent of the conformational free energy (i.e., J-factor). If δ is large, significant bending energy is alleviated at the transition state, so the barrier height depends on the bending energy. Thus, the looped lifetime dependence on the J-factor is largely dictated by the length scale of interaction, modulated in our model by δ.

The DNA mechanics are not solely a product of the bending energy, and over a short range of lengths, the twist resistance is the dominant energy that modulates the dynamic behavior. Small changes in length can have a large change on the total twist free energy by rotating the orientation out of phase by up to 180°. The twist free energy, like the binding energy, primarily affects the looped state. Our model results in the twist free energy turning on as the two ends start to feel one another, which is captured through an energetic penalty to the binding energy.

While we decouple the effects of twist from bending, we do recognize that such decoupling is not possible within experiments. The persistence length of DNA is affected by DNA sequence, yet these same changes in sequence can also affect the helical repeat length, which we assumed to be constant at 10.46 bp. The slight alterations in the locations of the peaks in the J-factor for different sequences in Johnson et al. (36,37) may be partially explained by changes in the helical repeat length. Despite this, the basic trend of the lifetime scaling over many decades should follow the scaling behavior without twist until the length is sufficiently long such that entropic effects become dominant over elastic contributions.

Finally, while our work has primarily been targeted to the looping of DNA in regulatory proteins, physical insights from this work are applicable to a broader range of problems involving DNA and synthetic polymers. Polymer looping is a general phenomenon important to a number of fields, and much work has been focused on looping within a biological context and in synthetic polymers (48). As in this work, the dynamics in these looping processes is controlled by the balance between the elastic behaviors of the polymers involved and the shape of the interaction that is binding the two distal regions of the polymer. Understanding the kinetics of DNA looping would be valuable in answering some of the fundamental questions underlying many cellular processes, including viral infection (49), the transmission of epigenetic marks (3), and the conformational changes in DNA that regulate gene expression.

AUTHOR CONTRIBUTIONS

P.J.M. designed research, performed research, contributed analytic tools, analyzed data, and wrote the article; Y.-J.C. and R.P. wrote the article; and A.J.S. designed research, performed research, contributed analytic tools, analyzed data, and wrote the article.

ACKNOWLEDGMENTS

This work was supported by the National Science Foundation, Physics of Living Systems Program under grant No. PHY-1305516 (to P.J.M. and A.J.S.); National Institutes of Health under Directors Pioneer Award No. DP1-OD000217A, grants No. R01-GM085286, No. R01-GM085286-01S1, and grant No. 1-U54-CA143869 (Northwestern Physical Sciences-Oncology Center); and the Fondation Pierre Gilles de Gennes (to Y.-J.C. and R.P.).

REFERENCES

1. Haber, J. E. 2012. Mating-type genes and MAT switching in *Saccharomyces cerevisiae*. *Genetics.* 191:33–64.
2. Shih, H.-Y., and M. S. Krangel. 2013. Chromatin architecture, CCCTC-binding factor, and V(D)J recombination: managing long-distance relationships at antigen receptor loci. *J. Immunol.* 190:4915–4921.
3. Grewal, S. I., and D. Moazed. 2003. Heterochromatin and epigenetic control of gene expression. *Science.* 301:798–802.
4. Postow, L., C. D. Hardy, …, N. R. Cozzarelli. 2004. Topological domain structure of the *Escherichia coli* chromosome. *Genes Dev.* 18:1766–1779.
5. Santo, K. P., and K. L. Sebastian. 2006. Opening of a weak link in a semiflexible ring polymer. *Phys. Rev. E Stat. Nonlin. Soft Matter Phys.* 73:031923.
6. Jun, S., J. Bechhoefer, and B. Y. Ha. 2003. Diffusion-limited loop formation of semiflexible polymers: Kramers theory and the intertwined time scales of chain relaxation and closing. *Europhys. Lett.* 64:420.

7. Chen, J. Z., H.-K. Tsao, and Y.-J. Sheng. 2005. Diffusion-controlled first contact of the ends of a polymer: crossover between two scaling regimes. *Phys. Rev. E Stat. Nonlin. Soft Matter Phys.* 72:031804.
8. Toan, N. M., G. Morrison, …, D. Thirumalai. 2008. Kinetics of loop formation in polymer chains. *J. Phys. Chem. B.* 112:6094–6106.
9. Wiggins, P. A., and P. C. Nelson. 2006. Generalized theory of semiflexible polymers. *Phys. Rev. E Stat. Nonlin. Soft Matter Phys.* 73:031906.
10. Afra, R., and B. A. Todd. 2013. Kinetics of loop formation in wormlike chain polymers. *J. Chem. Phys.* 138:174908.
11. Hyeon, C., and D. Thirumalai. 2006. Kinetics of interior loop formation in semiflexible chains. *J. Chem. Phys.* 124:104905.
12. Shore, D., J. Langowski, and R. L. Baldwin. 1981. DNA flexibility studied by covalent closure of short fragments into circles. *Proc. Natl. Acad. Sci. USA.* 78:4833–4837.
13. Du, Q., C. Smith, …, A. Vologodskii. 2005. Cyclization of short DNA fragments and bending fluctuations of the double helix. *Proc. Natl. Acad. Sci. USA.* 102:5397–5402.
14. Cloutier, T. E., and J. Widom. 2004. Spontaneous sharp bending of double-stranded DNA. *Mol. Cell.* 14:355–362.
15. Jacobson, H., and W. H. Stockmayer. 1950. Intramolecular reaction in polycondensations. I. The theory of linear systems. *J. Chem. Phys.* 18:1600–1606.
16. Finzi, L., and J. Gelles. 1995. Measurement of lactose repressor-mediated loop formation and breakdown in single DNA molecules. *Science.* 267:378–380.
17. Vanzi, F., C. Broggio, …, F. S. Pavone. 2006. Lac repressor hinge flexibility and DNA looping: single molecule kinetics by tethered particle motion. *Nucleic Acids Res.* 34:3409–3420.
18. Chen, Y. F., J. N. Milstein, and J. C. Meiners. 2010. FemtoNewton entropic forces can control the formation of protein-mediated DNA loops. *Phys. Rev. Lett.* 104:048301.
19. Laurens, N., D. A. Rusling, …, G. J. Wuite. 2012. DNA looping by FokI: the impact of twisting and bending rigidity on protein-induced looping dynamics. *Nucleic Acids Res.* 40:4988–4997.
20. Merlitz, H., K. Rippe, …, J. Langowski. 1998. Looping dynamics of linear DNA molecules and the effect of DNA curvature: a study by Brownian dynamics simulation. *Biophys. J.* 74:773–779.
21. Villa, E., A. Balaeff, and K. Schulten. 2005. Structural dynamics of the lac repressor-DNA complex revealed by a multiscale simulation. *Proc. Natl. Acad. Sci. USA.* 102:6783–6788.
22. Douarche, N., and S. Cocco. 2005. Protein-mediated DNA loops: effects of protein bridge size and kinks. *Phys. Rev. E Stat. Nonlin. Soft Matter Phys.* 72:061902.
23. Chen, Y.-J., S. Johnson, …, R. Phillips. 2014. Modulation of DNA loop lifetimes by the free energy of loop formation. *Proc. Natl. Acad. Sci. USA.* 111:17396–17401.
24. Saitô, N., K. Takahashi, and Y. Yunoki. 1967. The statistical mechanical theory of stiff chains. *J. Phys. Soc. Jpn.* 22:219–226.
25. Wiggins, P. A., T. van der Heijden, …, P. C. Nelson. 2006. High flexibility of DNA on short length scales probed by atomic force microscopy. *Nat. Nanotechnol.* 1:137–141.
26. Geggier, S., and A. Vologodskii. 2010. Sequence dependence of DNA bending rigidity. *Proc. Natl. Acad. Sci. USA.* 107:15421–15426.
27. Sinden, R. R. 1994. DNA Structure and Function. Gulf Professional Publishing, Houston, TX.
28. Spakowitz, A. J. 2006. Wormlike chain statistics with twist and fixed ends. *Europhys. Lett.* 73:684.
29. Spakowitz, A. J., and Z.-G. Wang. 2004. Exact results for a semiflexible polymer chain in an aligning field. *Macromolecules.* 37:5814–5823.
30. Spakowitz, A. J., and Z.-G. Wang. 2005. End-to-end distance vector distribution with fixed end orientations for the wormlike chain model. *Phys. Rev. E Stat. Nonlin. Soft Matter Phys.* 72:041802.
31. Mehraeen, S., B. Sudhanshu, …, A. J. Spakowitz. 2008. End-to-end distribution for a wormlike chain in arbitrary dimensions. *Phys. Rev. E Stat. Nonlin. Soft Matter Phys.* 77:061803.
32. Bryant, Z., M. D. Stone, …, C. Bustamante. 2003. Structural transitions and elasticity from torque measurements on DNA. *Nature.* 424:338–341.
33. Koslover, E. F., and A. J. Spakowitz. 2013. Discretizing elastic chains for coarse-grained polymer models. *Soft Matter.* 9:7016.
34. Koslover, E. F., and A. J. Spakowitz. 2013. Systemic coarse-graining of microscale polymer models as effective elastic chains. *Macromolecules.* 46:2003.
35. Risken, H. 1984. Fokker-Planck Equation. Springer, New York.
36. Johnson, S., M. Lindén, and R. Phillips. 2012. Sequence dependence of transcription factor-mediated DNA looping. *Nucleic Acids Res.* 40:7728–7738.
37. Johnson, S., Y.-J. Chen, and R. Phillips. 2013. Poly(dA:dT)-rich DNAs are highly flexible in the context of DNA looping. *PLoS One.* 8:e75799.
38. Shimada, J., and H. Yamakawa. 1984. Ring-closure probabilities for twisted wormlike chains. Application to DNA. *Macromolecules.* 17:689–698.
39. Allemand, J.-F., S. Cocco, …, G. Lia. 2006. Loops in DNA: an overview of experimental and theoretical approaches. *Eur. Phys. J. E Soft Matter.* 19:293–302.
40. Towles, K. B., J. F. Beausang, …, P. C. Nelson. 2009. First-principles calculation of DNA looping in tethered particle experiments. *Phys. Biol.* 6:025001.
41. Lewis, M., G. Chang, …, P. Lu. 1996. Crystal structure of the lactose operon repressor and its complexes with DNA and inducer. *Science.* 271:1247–1254.
42. Czapla, L., M. A. Grosner, …, W. K. Olson. 2013. Interplay of protein and DNA structure revealed in simulations of the lac operon. *PLoS One.* 8:e56548.
43. Kalodimos, C. G., N. Biris, …, R. Kaptein. 2004. Structure and flexibility adaptation in nonspecific and specific protein-DNA complexes. *Science.* 305:386–389.
44. van Valen, D., M. Haataja, and R. Phillips. 2009. Biochemistry on a leash: the roles of tether length and geometry in signal integration proteins. *Biophys. J.* 96:1275–1292.
45. Reeves, D., K. Cheveralls, and J. Kondev. 2011. Regulation of biochemical reaction rates by flexible tethers. *Phys. Rev. E Stat. Nonlin. Soft Matter Phys.* 84:021914.
46. Zhang, Y., A. E. McEwen, …, S. D. Levene. 2006. Analysis of in-vivo LacR-mediated gene repression based on the mechanics of DNA looping. *PLoS One.* 1:e136.
47. Rippe, K., P. H. von Hippel, and J. Langowski. 1995. Action at a distance: DNA-looping and initiation of transcription. *Trends Biochem. Sci.* 20:500–506.
48. Kricheldorf, H. R. 2010. Cyclic polymers: synthetic strategies and physical properties. *J. Polym. Sci. A Polym. Chem.* 48:251–284.
49. Griffith, J., A. Hochschild, and M. Ptashne. 1986. DNA loops induced by cooperative binding of lambda repressor. *Nature.* 322:750–752.